# Multivariate Autoregressive Independent Component Analysis for Real-Time Resting-State Functional Connectivity in High-Density EEG

K. Bagh<sup>1,2</sup>, S. Kopp<sup>2</sup> and A. Jahanian Najafabadi<sup>1</sup>

1. Dept. Cognitive Neuroscience, Bielefeld University, Bielefeld, Germany
2. Dept. of Technology, Bielefeld University, Bielefeld, Germany
khaled.bagh@uni-bielefeld.de, skopp@techfak.uni-bielefeld.de, amir.jahanian@uni-bielefeld.de

Abstract— In this study, we developed and evaluated a realtime implementation of the multivariate auto-regressive independent component analysis (MVARICA) model for estimating effective connectivity using Partial Directed Coherence (PDC). Each step of the MVARICA pipeline was adapted for online processing, with a focus on optimizing key hyperparameters, specifically model order and the delta ridge penalty in real time. The performance of the online model was benchmarked against a gold-standard offline MVARICA implementation. Our real-time model achieved a Mean Absolute Error (MAE) of 0.070 (7% error), with 95% of the value falling within a 20% deviation from the offline reference. Errors varied across frequency bands: Delta (MAE = 11.5%), Theta (9.1%), Alpha (7.8%), Beta (5.5%), and Gamma (3.6%). The Pearson correlation across all frequency bands exceeded 0.744, indicating strong agreement between the online and offline models. The real-time model successfully captured the key connectivity patterns identified by the offline version, converged reliably on hyperparameter optimization, and operated within real-time constraints for a low number of channels. Specifically, latency remained under 100 ms for low channel inputs but increased to approximately 1 second for high-density configurations.

Keywords—EEG, Resting-state Functional Connectivity, MVARICA, CNN, and Deep Learning.

## I. INTRODUCTION

Electroencephalography (EEG) is a non-invasive neuroimaging technique known for its high temporal resolution, widely used to study neural dynamics in neurological, developmental, and psychological disorders. Its ability to capture real-time electrical activity across the scalp makes EEG particularly valuable for brain–computer interfaces (BCIs) and assistive therapeutic technologies [1–4]. EEG enables real-time monitoring of neuronal oscillations and thus serves as a fundamental tool for neurofeedback and clinical diagnostics [5, 6].

A central method for interpreting EEG data is functional connectivity (FC), which quantifies statistical dependencies between distributed brain regions. While directed FC measures such as Granger causality and Partial Directed Coherence (PDC) estimate causal information flow in the frequency domain [7, 8], their computation is traditionally offline and computationally demanding. Moreover, methods combining Multivariate Autoregressive (MVAR) modeling with Independent

Component Analysis (ICA), known as MVARICA, have shown promise in improving interpretability and reducing artifacts such as volume conduction [9]. However, despite their utility, existing MVARICA implementations remain limited to offline processing, making them unsuitable for real-time or closed-loop applications where immediate feedback is essential.

In this study, we address this critical limitation by introducing a novel real-time implementation of MVARICA for estimating resting-state directed functional connectivity from high-density EEG. The proposed framework transforms the conventional offline MVARICA pipeline into an online, adaptive system optimized for low-latency processing. Specifically, each step of the MVARICA model—MVAR coefficient estimation, ICA decomposition, and PDC computation—has been reengineered for real-time operation through algorithmic and computational optimizations.

This real-time design enables dynamic tracking of brain network interactions with short update intervals (<250 ms) with large data window (e.g. 2 seconds), bridging the gap between advanced EEG connectivity modeling and real-time applications such as neurofeedback and adaptive BCIs. This work is the first real-time framework and validation of MVARICA for directed functional connectivity in EEG in real-time, offering a complete redesign of the MVARICA pipeline for real-time operation, algorithmic innovations that enable stable, low-latency estimation of brain network dynamics, it also demonstrated the feasibility for integration into closed-loop BCI and neurofeedback systems where immediate, causal feedback is required.

## II. BACKGROUND

The foundation of MVARICA originates from Auto-Regressive (AR) models, which describes the current value of a signal as a linear combination of its past values. For EEG data, the model MVAR was used, as to account for the multi-channel nature of the EEG data. The MVAR model for a signal of N time points and M channels is described in (1).

$$X(t) = \sum_{k=1}^{p} A(k).X(t-k) + E(t)$$
 (1)

where X(t) is a vector of size M, at time point t, p, which is a model hyperparameter called model order, is the

number of past time points used to predict the current time point t, and A(k) is the model coefficients, of dimensions (M, M). E(t) is the error vector, of size M. The AR coefficients are estimated using methods such as the Yule-Walker equations or least squares optimization [10]. The coefficients then served as the foundation for computing the connectivity by applying the Fourier transform to the coefficients. From the transformed coefficients, connectivity metrics like PDC [11] can be computed, as in (2).

$$PDC_{ij}(f) = \frac{B_{ij}(f)}{\sqrt{\sum_{k=1}^{N} \left|B_{ij}(f)\right|^2}}$$
 (2)

where i and j are two EEG channels and N is the number of channels.

A distinctive feature of the MVARICA model was the application of Independent Component Analysis (ICA) on the residuals in the time domain to extract latent channel patterns not captured by the MVAR coefficients. These residual patterns were assumed to be non-Gaussian and statistically independent, making ICA a natural choice. Using the mixing and unmixing matrices derived from the ICA decomposition, we updated the MVAR coefficients to reflect contributions from the independent sources.

To prevent overfitting the model coefficients to the data, we employed delta ridge regression [12], which incorporated a regularization parameter,  $\delta$ . This parameter played a critical role in stabilizing the solution, particularly when the number of time points was limited or the predictors were highly collinear—a typical scenario in EEG data. We optimized two key hyperparameters—model order and  $\delta$ —for accurate model performance. Model orders were selected using techniques such as leave-one-out cross-validation (LOOCV), which minimized the mean squared generalization error, or by minimizing the Akaike Information Criterion (AIC). The  $\delta$  parameter was optimized using the bisection search method [13]. However, these conventional optimization strategies were not well-suited for real-time applications due to their computational demands.

## III. MATERIALS AND METHODS

To adapt the MVARICA model for real-time applications, we modified the algorithm to operate within real-time constraints and optimized its hyperparameters during execution. Our objective was to run the complete MVARICA pipeline under 250 ms, even under varying computational stress conditions. A chart of the original offline algorithm is illustrated in Fig. 1, the primary computational bottlenecks in the model included the initial estimation of MVAR coefficients, fitting the ICA on the residuals, and computing the PDC.

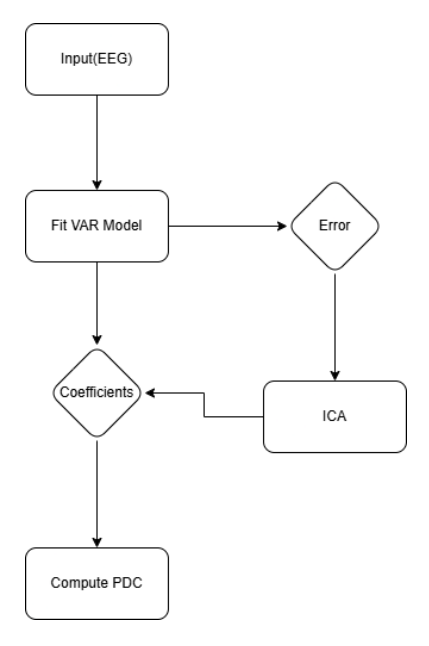


Figure 1. Flowchart of MVARICA.

The offline model coefficients were computed using a least-squares solution. This was replaced by incremental QR updates based on Givens rotations [14]. The QRbased approach offers superior computational efficiency and numerical stability compared to solving the leastsquares problem via the normal equations. Moreover, it aligns well with the real-time requirements of the system. In scenarios involving high window overlap—such as computing PDC on a 2-second window with 90% overlap, which is common in functional connectivity analyses—the majority of the data remains unchanged between successive windows. The incremental method leverages this by updating only the necessary ranks and discarding outdated ones, thereby optimizing performance for real-time applications.

To modify the ICA step in the MVARICA, it is important to pick a method that is appropriate and fast. Several methods were considered, like Second Order Blind Identification (SOBA) [15], Independent Vector Analysis (IVA) [16], or Sparse ICA (SICA) [17]. However, IVA assumes the sources are Gaussian, and SOBA also assumes the sources are not independent and non-Gaussian. While SICA does take an independent and non-Gaussian source, the residual cannot be considered sparse. An appropriate method was Orthogonal-Preconditioned ICA for Real Data (O-PICARD) [18, 19], which makes the same assumptions as regular ICA (FAST-ICA). As part of the MVAR coefficient update from the ICA, we leveraged the iterative nature of our application. Specifically, we used the unmixing matrix from the previous iteration as the initial guess for the subsequent iteration to O-PICARD, to accelerate convergence and improve computational efficiency.

The computation of the PDC was kept the same, as the PDC computation complexity is not related to the length of the data; instead, it is affected by the number of EEG channels and the model order.

To enable real-time hyperparameter optimization, we implemented two distinct methods-one for each hyperparameter: model order and the delta regularization parameter. To optimize the model order, we introduced a Recursive-AIC (RAIC) method, as outlined in Algorithm 1. The approach was based on minimizing the AIC score, similar to traditional offline approaches; however, the search window was significantly reduced to support realtime performance. The core idea was to allow the model order to converge gradually over time rather than search exhaustively at every step. We employed an adaptive search window strategy guided by the heuristic: "If the underlying stationary characteristics of the signal do not change substantially, the optimal model order is unlikely to shift significantly." To quantify such changes, we maintained a running history of the signal's mean and standard deviation. If the current mean or standard deviation exceeded a predefined percentile threshold (e.g., the 90th percentile) of this historical distribution, the search window was dynamically expanded, allowing for faster convergence in response to more substantial shifts in signal properties.

To optimize the delta hyperparameter, we used the standard ADAM optimizer [20], where the loss was computed from the Mean Squared Error (MSE) of the residual.

#### IV. EXPERIMENTAL SETUP

To evaluate the model, there are three aspects to validate:

- 1. How accurate is the online system?
- 2. How well does it optimize the hyperparameters?
- 3. How fast is it?

In order to evaluate the first question, we compared our real-time online model with an offline model. The offline model was based on our previous work [21, 21], which is based on the SCOT package implementation [9]. The comparison between the two models is done under the same hyperparameter conditions (i.e., no optimization was performed). To evaluate the second question, each hyperparameter optimization method was assessed independently, where we tested each method for accuracy, convergence, and stability. The third question was tested under different conditions of stress, using different number of channels and different overlap percentages.

The dataset used in this study was obtained from the Healthy Brain Network (HBN) initiative [22]. We selected 265 resting-state EEG recordings from healthy children and adolescents aged 5 to 21 years. The data

Algorithm 1 RAIC: Rolling AIC-based model order adaptation

```
1: procedure RAIC(X, mean_hist, std_hist, cur-
    rent_order, change_percentile)
        mean_t \leftarrow mean(X)
        std_t \leftarrow std(X)
 3:
 4:
        roll\_mean \leftarrow |mean_t - mean_{t-1}|
        roll \ std \leftarrow |std_t - std_{t-1}|
 5:
        eps\_mean \leftarrow percentile(mean\_hist, change\_percentile)
        eps\_std \leftarrow percentile(std\_hist, change\_percentile)
        Append roll_mean to mean_hist
        Append roll_std to std_hist
                                          (roll_mean
        is_nonstationary
10:
                                                            >
    eps\_mean) or (roll\_std > eps\_std)
11:
        if is_nonstationary then
            search window \leftarrow 5
12:
13:
            search\_window \leftarrow 1
14:
15:
        end if
        best aic \leftarrow \infty
16:
        for p in (current_order - search_window) to
    (current_order + search_window) do
18:
             Attempt to fit MVAR model of order p
             if model fitting fails then
19:
20:
                aic \leftarrow \infty
21:
             else
                 aic \leftarrow AIC of fitted model
22.
             end if
24:
             if aic < best_aic then
25:
                 best\_aic \leftarrow aic
26:
                 best\_order \leftarrow p
27:
            end if
        end for
28:
        return best_order
30: end procedure
```

were recorded at a sampling rate of 500 Hz with a bandpass range of 0.1-100 Hz, using a 128-channel HydroCel Geodesic EEG system (Electrical Geodesics Inc.). After excluding outer electrodes, 109 channels were retained for analysis. The scalp distribution of the electrodes is shown in Fig. 2. Offline pre-processing was performed following the pipeline established in our previous work [21, 21, 23]. The PREP pipeline [24] was used to detect and interpolate bad channels. The data were then band-pass filtered between 1-70 Hz and notch filtered at 60 Hz to remove power line noise. After resampling to 256 Hz, the signals were re-referenced to the average of all channels. Finally, artifact removal was performed using the FAST-ICA algorithm. Although this pre-processing was conducted offline, several studies have demonstrated the feasibility of implementing these steps in real-time [25, 26]. For this study, however, our primary goal was to enable a fair comparison with a goldstandard offline model, starting from similar preprocessed input data.

The online MVARICA framework was implemented using the O-PICARD algorithm for independent component extraction, with a maximum of 10 iterations and a convergence tolerance of 0.0001. Both the online

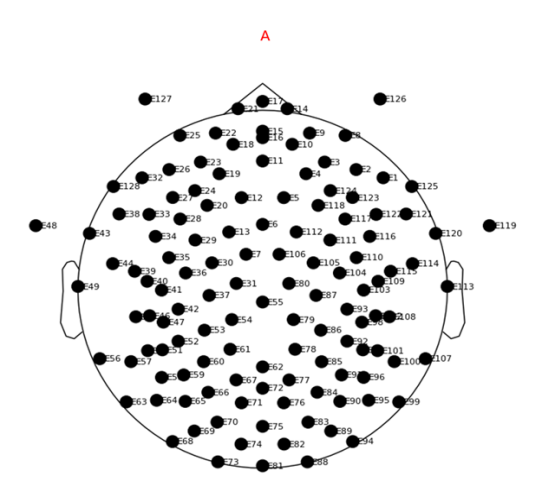


Figure 2. Channel location of 128-channels in the dataset

and offline models were evaluated using 2-second, non-overlapping EEG windows. To investigate model accuracy, model orders were varied from 1 to 30 in increments of 3. To reduce computational load, the analysis focused on 12 EEG channels located primarily in the right frontal region (E1, E2, E3, E4, E5, E8, E9, E10, E14, E118, E123, and E124). The ridge regularization parameter ( $\delta$ ) was fixed at 0.12 for this comparison. PDC values were computed and averaged across standard EEG frequency bands: Delta (1–4,Hz), Theta (4–8,Hz), Alpha (8–12,Hz), Beta (12–30,Hz), Gamma (30–70,Hz), and the broadband range (1–70,Hz).

For hyperparameter optimization, the same 2-second segmentation approach was applied. The offline model optimized model order independently for each segment, while the online model dynamically tested initial orders from 1 to 30 (step size = 3) using a fixed  $\delta$  = 0.12. Online  $\delta$  optimization was implemented exclusively in the realtime model. The algorithm was initialized with  $\delta$  values of 0.1, 5, 20, and 50, while keeping the model order fixed at 1. The Adam optimizer was employed with learning rates of 3, 0.1, and 0.001, and with momentum parameters  $\beta 1 = \beta 2 = 0.6$ . A direct comparison of  $\delta$ optimization between the online and implementations was not pursued, as  $\delta$  primarily serves as a stability parameter rather than a major driver of connectivity differences. The focus was instead on verifying stable convergence to practical  $\delta$  values suitable for real-time use.

System latency was evaluated to assess real-time performance under different computational loads. The online model was executed using both the 12-channel subset and the full 109-channel configuration. Data intake was updated every 250 ms, with window overlaps of 75% (effective 1-second window) and 87.5% (effective 2-second window). The PDC resolution was set to nfft = 500 in all tests unless otherwise specified.

All experiments were conducted on Google Colab using an NVIDIA L4 GPU, with GPU acceleration handled through the CuPy library in Python 3.11.13.

## V. EXPERIMENTAL RESTULS

To evaluate the accuracy of the online model and its consistency with the offline model, we calculated the Mean Absolute Error (MAE) between their respective PDC values. The MAE was 0.070, indicating a 7% average deviation between the two models. Additionally, the Pearson correlation coefficient was 0.910 (p < 0.001), suggesting a very strong agreement in the features detected by both models.

To further assess their overall agreement, we used a Bland-Altman plot (Fig. 3). The mean difference between the online and offline PDC values was 0.009, indicating no significant systematic bias. The 95% limits of agreement ranged from -0.188 to 0.206. Fig. 4 illustrates the relationship between frequency bands and model order. For lower frequencies, particularly in the delta band, lower model orders yield better MAE scores, suggesting that simpler models are more effective in capturing low-frequency dynamics. In contrast, midrange frequencies such as theta and alpha exhibit relatively stable MAE values across different model

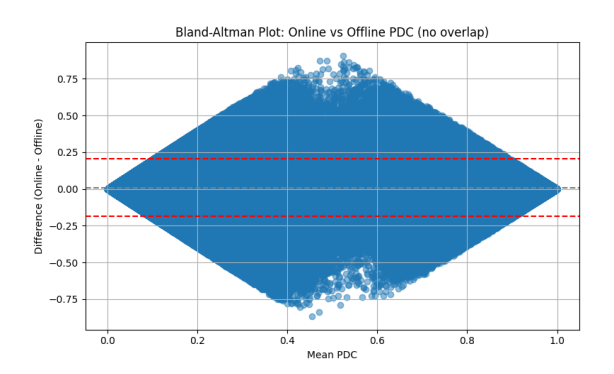


Figure 3. Bland-Altman plot for the online and offline models. The res lines are the 95<sup>th</sup> percentile of the agreement. The gray dotted line is the mean of the agreement.

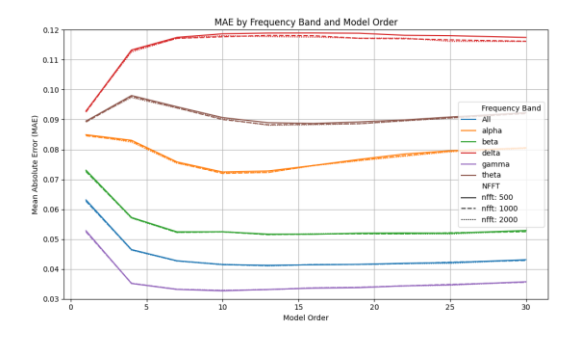


Figure 4. MAE score based on the different model order, under different frequency ranges.

orders, indicating minimal sensitivity to model complexity. For higher frequency bands, including beta, gamma, and the full spectrum, the MAE improves as model order increases, eventually reaching a plateau. This suggests that higher model orders are necessary to accurately capture the complexity of high-frequency interactions, but beyond a certain point, additional complexity offers diminishing returns.

The optimization results for model order are presented in Fig. 5. As shown, the online model consistently converges toward the optimal model order range identified by the offline model and remains within that range throughout, demonstrating stable and reliable adaptation.

Fig. 6 illustrates the convergence behavior of the delta parameter under different learning rates of the Adam optimizer. Results revealed that when the initial delta value is far from optimal, a higher learning rate is

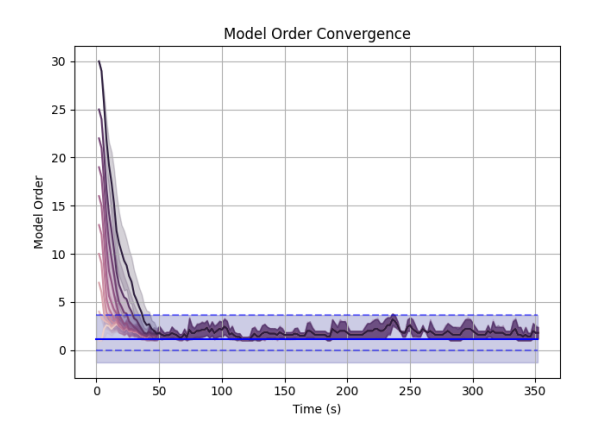


Figure 5. Model order convergence of RAIC, where the blue line shows the mean of the optimal selected model order of the offline model, the two shaded lines show the upper standard deviation and the zero line.

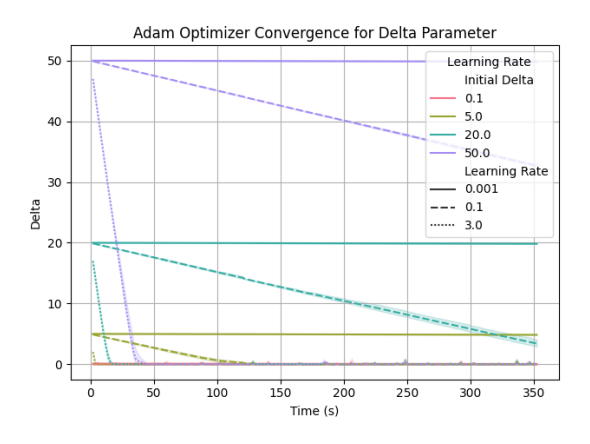


Figure 6. Delta convergence with Adam optimizer, under different learning rate and starting values of delta.

necessary to accelerate convergence. Nevertheless, across all tested conditions, the Adam optimizer consistently guides the delta parameter toward stable and reasonable values, particularly suited for resting-state EEG data segmented into 2-second windows.

Fig. 7 illustrates the convergence behavior of delta under different learning rates, where the initial delta was set to 0.1. A high learning rate (lr = 3) introduces significant noise, resulting in unstable delta values, whereas lower learning rates lead to more stable and consistent convergence.

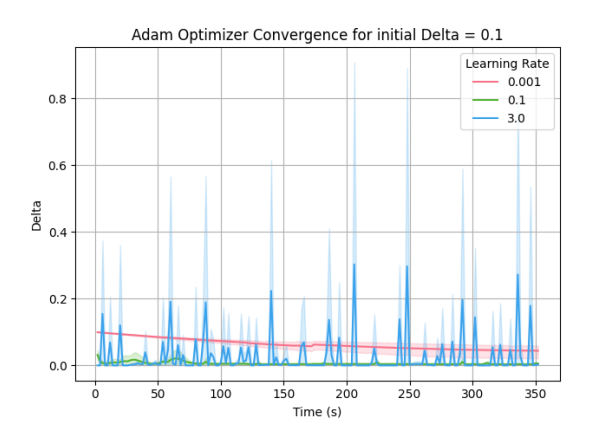


Figure 7. Delta convergence with Adam optimizer, under different learning rates for starting delta of 0.1.

Table 1 presents the latency performance of the online model under various stress conditions. Results further revealed that when using 12 channels, the model maintains acceptable latency—remaining below the 250 ms threshold—even as the overlap increases, indicating that overlap does not significantly impact performance in this configuration. However, when the number of channels is increased to 109, latency exceeds 250 ms, demonstrating that the model no longer meets real-time processing requirements under this higher computational load. Fig. 8 shows the performance of the online model under different model orders and stress conditions.

# VI. DISCUSSION

The proposed real-time MVARICA framework demonstrated strong agreement with the offline reference

Table 1. shows the performance of the online model under different model orders and stress conditions.

		MVAR		Packet	Optim.	
Chan.	Over-	fitting	ICA	process.	step	Time
Num.	lap	(ms)	(ms)	(ms)	(ms)	(ms)
12	75%	10.6	30.5	41.9	44.6	86.7
12	87.5%	10.6	32.8	44.2	44.6	88.8
109	75%	92.6	523.4	643.0	291.5	934.5
109	87.5%	99.5	699.4	826.5	296.0	1222.5

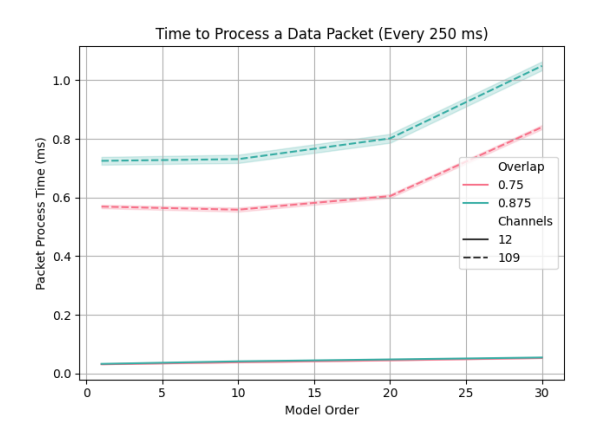


Figure 8. Latency under different model orders and different stress conditions.

model, achieving a MAE of 7%, with 95% of PDC values differing by less than 0.2. Although slightly higher discrepancies were observed in the delta band (MAE = 11.5%), the overall correlation remained high (Pearson r = 0.744), indicating that the online model reliably captured the major directed connectivity patterns detected offline. This level of accuracy is acceptable for real-time neurofeedback and BCI applications, where small deviations are tolerable in exchange for lowlatency processing. The increased delta-band error is consistent with known limitations in low-frequency connectivity estimation, where fewer oscillatory cycles within short time windows increase susceptibility to noise and temporal instability. Hence, the observed differences reflect the intrinsic difficulty of modeling slow oscillations rather than a shortcoming of the online approach.

The frequency-dependent behavior observed in Fig. 4 further supports this interpretation. Delta-band activity (1–4 Hz) typically requires longer analysis windows (10– 20 s) and higher model orders (20-30) for accurate representation in offline conditions. In this study, both models operated on 2-second windows to meet real-time constraints, capturing only a few oscillatory cycles. Under such conditions, higher model orders tend to become numerically unstable, increasing estimation variance. Conversely, lower model orders provided more stable estimates, reducing overfitting. In higher frequency ranges (e.g., beta and gamma), where more cycles are contained within the same time window, model stability improves, and the online and offline estimates align closely. Importantly, the online modelmaintained flexibility for extending window duration when computational resources allow, providing a tunable balance between temporal precision and frequency resolution.

The adaptive model-order optimization method, RAIC, consistently converged toward the range identified by the

offline model (Fig. 5), confirming its ability to track optimal model complexity in real time. The relatively stable convergence reflects the resting-state nature of the dataset, where minimal non-stationarity reduces the need for frequent adaptation. However, convergence speed can vary depending on initialization; when the starting model order deviates substantially from the optimal value, convergence may take up to 50 seconds. To enhance responsiveness under non-stationary or task-related conditions, a two-stage adaptation strategy is recommended: an initial broad search window during early model stabilization, followed by an adaptive narrowing phase once stationarity is achieved. This hybrid approach could improve both accuracy and adaptability for dynamic EEG paradigms.

Similarly, the  $\delta$ -parameter optimization using the Adam algorithm showed stable convergence across conditions (Fig. 6), though convergence speed was influenced by initialization and learning rate. High learning rates accelerated adaptation but occasionally produced oscillatory behavior or overshooting (Fig. 7). A progressive learning-rate schedule—starting high and gradually decreasing once stability is achieved—could mitigate this trade-off. Such a configuration would ensure rapid yet stable optimization, which is particularly valuable in real-time neurofeedback applications where responsiveness to changing brain states is critical.

Latency analysis confirmed that the number of EEG channels was the primary determinant of computational delay. With 12 channels, total latency remained below 100ms, well within real-time constraints for neurofeedback and closed-loop BCI operation. However, processing high-density EEG (109 channels) increased latency to approximately 1 s, primarily due to the ICA and optimization steps. While this exceeds the strict real-time threshold, it remains acceptable for semi-online analysis or slower feedback loops. In typical neurofeedback systems that rely on fewer than 10 channels, the proposed framework comfortably supports real-time performance.

Future work could further reduce latency by incorporating dimensionality-reduction techniques—such as Principal Component Analysis (PCA) or autoencoder-based embeddings—to preserve essential signal characteristics while reducing computational load. Such strategies could enable scalability to high-density EEG without compromising timing requirements.

Overall, these results establish the proposed real-time MVARICA framework as a proof of concept that achieves a practical balance between computational efficiency, modeling accuracy, and system responsiveness. The implementation demonstrates the feasibility of translating complex offline connectivity analyses into an adaptive, low-latency pipeline suitable

for closed-loop neurofeedback and BCI applications. As a foundational prototype, the current system provides evidence that real-time directed connectivity estimation from EEG is technically viable, while also revealing key areas for improvement. Future work should extend this framework beyond resting-state data to event-related and task-based EEG, where transient neural responses and rapid state changes pose additional challenges for online modeling. Enhancements in adaptive hyperparameter control, dimensionality reduction, and dynamic windowing strategies will further strengthen the scalability and robustness of real-time MVARICA in large-scale cognitively demanding neurophysiological contexts.

### VII. CONCLUSIONS

This study introduced a novel real-time implementation of the Multivariate Autoregressive Independent Component Analysis (MVARICA) framework for estimating directed functional connectivity from highdensity EEG. The proposed system successfully translated the traditionally offline MVARICA pipeline into a fully online, adaptive model capable of computing Partial Directed Coherence (PDC) in real time. The online implementation demonstrated strong agreement with its offline counterpart, achieving a mean absolute error of 7% while maintaining stable convergence of key hyperparameters, including model order regularization strength.

Although full real-time performance with 109 EEG channels remains computationally demanding, the framework operated reliably and within real-time constraints using a 12-channel configuration. These results confirm the feasibility of applying advanced connectivity modeling in low-latency applications such as closed-loop brain-computer interfaces (BCIs) and neurofeedback systems. The use of GPU acceleration (NVIDIA L4) enabled high-throughput computation, positioning the current implementation as a practical solution for laboratory and clinical research environments.

### **ACKNOWLEDGMENTS**

This manuscript was prepared using limited access to the datasets obtained from the USA BioBank provided by Child Mind Institute (CMI), Healthy Brain Network. This manuscript reflects the views of the authors and does not necessarily reflect the opinions or views of the CMI. BioBank access was granted to Dr. Amir Jahanian Najafabadi under the official agreement signed by Bielefeld University.

#### REFERENCES

- [1] C. Bhaskarachary, A. J. Najafabadi, and B. Godde, "Machine learning supervised classification methodology for autism spectrum disorder based on resting-state electroencephalography (eeg) signals," 2020 IEEE Signal Processing in Medicine and Biology Symposium (SPMB). IEEE, 2020, pp. 1–4.
- [2] G. Ciodaro, A. J. Najafabadi, and B. Godde, "Resting state eeg classification of children with adhd," 2020 IEEE Signal Processing in Medicine and Biology Symposium (SPMB). IEEE, 2020, pp. 1–6.
- [3] S. Lopez, G. Suarez, D. Jungreis, I. Obeid, and J. Picone, "Automated identification of abnormal adult eegs," 2015 IEEE signal processing in medicine and biology symposium (SPMB). IEEE, 2015, pp. 1–5.
- [4] V. Shah, M. Golmohammadi, S. Ziyabari, E. Von Weltin, I. Obeid, and J. Picone, "Optimizing channel selection for seizure detection," 2017 IEEE signal processing in medicine and biology symposium (SPMB). IEEE, 2017, pp. 1–5.
- [5] H. Zhang, L. Jiao, S. Yang, H. Li, X. Jiang, J. Feng, S. Zou, Q. Xu, J. Gu, X. Wang, and B. Wei, "Brain-computer interfaces: the innovative key to unlocking neurological conditions," International Journal of Surgery, vol. 110, no. 9, pp. 5745–5762, September 2024.
- [6] X. Liu, W. Wang, M. Liu et al., "Recent applications of eeg-based brain-computer-interface in the medical field," Military Medical Research, vol. 12, p. 14, 2025. (available at: https://doi.org/ 10.1186/s40779-025-00598-z).
- [7] A. M. Bastos and J. Schoffelen, "A tutorial review of functional connectivity analysis methods and their interpretational pitfalls," Frontiers in Systems Neuroscience, vol. 9, 2016. (available at: https://doi.org/10.3389/ fnsys.2015.00175).
- [8] S. L. Bressler, A. Kumar, and I. Singer, "Brain synchronization and multivariate autoregressive (mvar) modeling in cognitive neurodynamics," Frontiers in Systems Neuroscience, vol. 15, p. 638269, 2022. (available at: https://doi.org/10.3389/fnsys. 2021.638269).
- [9] M. Billinger, C. Brunner, and G. R. Müller-Putz, "Scot: a python toolbox for eeg source connectivity," Frontiers in neuroinformatics, vol. 8, p. 22, 2014.
- [10] L. Kilian, "New introduction to multiple time series analysis, by helmut lütkepohl, springer, 2005," Econometric theory, vol. 22, no. 5, pp. 961–967, 2006.
- [11] L. A. Baccalá and K. Sameshima, "Partial directed coherence: a new concept in neural structure determination," Biological cybernetics, vol. 84, no. 6, pp. 463–474, 2001.
- [12] P. Patil, J.-H. Du, and R. J. Tibshirani, "Optimal ridge regularization for out-of-distribution prediction," arXiv preprint arXiv:2404.01233, 2024.
- [13] M. A. van de Wiel, M. M. van Nee, and A. Rauschenberger, "Fast cross-validation for multi-penalty high-dimensional ridge regression," Journal of Computational and Graphical Statistics, vol. 30, no. 4, pp. 835–847, 2021.
- [14] D. Olteanu, N. Vortmeier, and Živanovi'c, "Givens rotations for qr decomposition, svd and pca over database joins," The VLDB Journal, vol. 33, no. 4, pp. 1013–1037, 2024.
- [15] Y. Pan, M. Matilainen, S. Taskinen, and K. Nordhausen, "A review of second-order blind identification methods," Wiley interdisciplinary reviews: computational statistics, vol. 14, no. 4, p. e1550, 2022.
- [16] T. Kim, I. Lee, and T.-W. Lee, "Independent vector analysis: Definition and algorithms," 2006 Fortieth Asilomar Conference on Signals, Systems and Computers. IEEE, 2006, pp. 1393–1396.

- [17] A. M. Bronstein, M. M. Bronstein, M. Zibulevsky, and Y. Y. Zeevi, "Sparse ica for blind separation of transmitted and reflected images," International Journal of Imaging Systems and Technology, vol. 15, no. 1, pp. 84–91, 2005.
- [18] G. Frank, S. Makeig, and A. Delorme, "A framework to evaluate independent component analysis applied to eeg signal: testing on the picard algorithm," 2022 IEEE International Conference on Bioinformatics and Biomedicine (BIBM). IEEE, 2022, pp. 2009– 2016.
- [19] I. Biswas and T. L. Gómez, "Hecke transformation for orthogonal bundles and stability of picard bundles," arXiv preprint arXiv:1103.0870, 2011.
- [20] D. P. Kingma and J. Ba, "Adam: A method for stochastic optimization," arXiv preprint arXiv:1412.6980, 2014.
- [21] A. J. Najafabadi and K. Bagh, "Resting-state functional connectivity in children and adolescents with major depressive disorder: A deep learning approach using high-density eeg," 2024 IEEE Signal Processing in Medicine and Biology Symposium (SPMB). IEEE, 2024, pp. 1–7.
- [22] L. M. Alexander, J. Escalera, L. Ai, C. Andreotti, K. Febre, A. Mangone, N. Vega-Potler, N. Langer, A. Alexander, M. Kovacs et al., "An open resource for transdiagnostic research in pediatric mental health and learning disorders," Scientific data, vol. 4, no. 1, pp. 1–26, 2017.
- [23] A. J. Najafabadi and K. Bagh, "Deep learning analysis approach for major depressive disorder in children and adolescents," Preprint, 2024.
- [24] C. Craddock, S. Sikka, B. Cheung, R. Khanuja, S. S. Ghosh, C. Yan, Q. Li, D. Lurie, J. Vogelstein, R. Burns et al., "Towards automated analysis of connectomes: The configurable pipeline for the analysis of connectomes (c-pac)," Front Neuroinform, vol. 42, no. 10.3389, 2013.
- [25] S.-H. Hsu, T. R. Mullen, T.-P. Jung, and G. Cauwenberghs, "Real-time adaptive eeg source separation using online recursive independent component analysis," IEEE transactions on neural systems and rehabilitation engineering, vol. 24, no. 3, pp. 309– 319, 2015.
- [26] V. Zotev, R. Phillips, H. Yuan, M. Misaki, and J. Bodurka, "Self-regulation of human brain activity using simultaneous real-time fmri and eeg neurofeedback," NeuroImage, vol. 85, pp. 985–995, 2014.